Molecular dynamics during linear chain polymerization from real-time dielectric spectrometry and calorimetry

1997 J. Phys.: Condens. Matter 9 7017

(http://iopscience.iop.org/0953-8984/9/33/006)

J. Phys.: Condens. Matter **9** (1997) 7017–7037. Printed in the UK PII: S0953-8984(97)81258-1

Molecular dynamics during linear chain polymerization from real-time dielectric spectrometry and calorimetry

E Tombari†, C Ferrari†, G Salvetti† and G P Johari‡

† Istituto Fisica Atomica e Molecolare del CNR, via del Giardino 7, 56127-Pisa, Italy
‡ Department of Materials Science and Engineering, McMaster University, Hamilton, Ontario L8S 4L7, Canada

Received 24 January 1997, in final form 7 May 1997

Abstract. To obtain physical insight into the slowing of the molecular dynamics when a macromolecule grows as a result of polymerization, (i) the dielectric relaxation spectra, and (ii) the heat evolved during the growth of a linear chain structure by means of the reaction of diepoxide with a monoamine have been measured simultaneously and continuously over time, at a fixed temperature of 314.2 K, during fixed-rate heating to 341.5 K and thereafter cooling from this temperature. An instrument was designed for the purpose. The studies yield information, almost simultaneously, on the changes in the dc conductivity, on the static and dynamic behaviours of the dipolar relaxation, and on the number of covalent bonds, n, in the states of the structures formed by irreversible polymerization. The dc conductivity decreases with increase in n, but this decrease cannot be attributed entirely to the increase in viscosity. The decrease in the ion population has a significant effect on the change in dc conductivity. Both the equilibrium permittivity and the limiting high-frequency permittivity decrease on polymerization. This decrease is attributed mainly to a decrease in the dipolar orientational correlation factor in the former case, and to a predominant increase in the phonon frequencies in the latter case. It is found that the slowing of the molecular dynamics that occurs here on increase in n is more than compensated by the acceleration of the dynamics on increase in the thermal energy. This effect is interpreted in terms of the changes in the configurational entropy, S_{conf}, which leads to relations expressing the dependence of S_{conf} on n, as well as on the temperature. A faster molecular dynamics of the Johari–Goldstein relaxation evolves as n increases. This dynamics does not depend on the decrease in S_{conf} with decrease in n, but depends only on the change in S_{conf} with temperature. The dielectric behaviour of the completely polymerized state obtained after repeated thermal cycling of the initially molecular liquid has been studied, and the results are related to the molecular dynamics observed during the growth of the macromolecules.

1. Introduction

During the process of polymerization, molecules in the initially molecular state of a liquid chemically combine to form bigger molecules. The product, which is obviously bigger in size than the reactants, diffuses at a slower rate than either one of the reactants. This causes the rate of chemical combination to become slower. Hence, any further chemical combination that occurs is affected by this slower rate, and, after the combination has occurred, the product is a yet bigger macromolecule, which diffuses even more slowly. This continues until both the diffusion and the chemical combination rate, after slowing each other progressively more, become too slow to be experimentally observable. At this instant, the process seems to come to a virtual halt, within the timescale of one's observation. When the liquid's viscosity has reached a certain high value and the diffusion coefficient

0953-8984/97/337017+21$19.50

a certain low value, the liquid is said to have vitrified, almost isothermally. This process of a negative feedback [1] between the chemical combination that increases the molecular size and the diffusion, which slows the rate of the very process that causes this increase in size, is usually studied as a function of time, and explained in the reaction time domain [1–12]. To gain physical insight into the molecular dynamics of such processes, more recent studies [13–17] have attempted to change the manner in which the process is viewed, by interpreting it in terms of the number of covalent bonds formed; these bonds increase the configurational restrictions on molecular diffusion. If this is done, the molecular dynamics of the process can be related to an intrinsic property of the structure of the liquid, rather than to an extrinsic property such as the time allowed for chemical combination. To gain further insight into the physics of the process in which a negative feedback between the chemical combination and the molecular dynamics is predominant, we have made a detailed study of a linear chain macromolecule during the course of its formation and growth by polymerization, which is reported here.

The growth of a macromolecule over time has been studied by a variety of techniques, namely, those of ultrasonic relaxation [4–6], dynamic heat capacity [18], density [8, 9], calorimetry [19, 20], vibrational spectroscopy [4, 7], viscosity [3] and dielectric relaxation [1, 2, 9, 10]. Amongst these, the dielectric spectroscopy technique appears to be the most sensitive and easily adaptable one. But, as in all studies of this type, it has not been possible to measure simultaneously the dielectric spectra and thermal behaviour of the same sample continuously over time. Therefore, to study the physical aspects of this process, it was necessary to develop a measurement assembly for the purpose. This is also briefly reported here. In the main, this paper describes a study of how the molecular dynamics in a liquid changes when macromolecular growth occurs in it, or the number of covalent bonds formed in its continuously changing structure increases spontaneously over time. The study also reveals how new relaxation processes evolve, and how the increase in the thermal energy of the system effectively compensates for the configurational restrictions imposed by the growing molecular size. Finally, we provide a dielectric study of the polymerized product ultimately formed, and of its relationship with the processes that led to the formation of this product. Although restricted to one system, the physics described here is likely to be useful generally, for all processes in which the slowing of the molecular dynamics is caused by the spontaneous growth of macromolecules.

2. Experimental methods

The polymerization was achieved in a liquid mixture containing a diepoxide and a monoamine mixed in equimolar amounts. The reaction between the two leads to the formation of mainly a linear chain polymer. Cyclohexylamine (99% purity) was purchased from Aldrich Chemicals, and diglycidyl ether of bisphenol-A (DGEBA) was obtained from Shell Chemicals. The latter had the trade name of EPON 828 EL. Its number average molecular weight is 380 Dalton, the average number of repeat units in the molecule is 0.14, which indicates that the size of any oligomers is negligibly small, its glass transition temperature is 259 K, and its functionality (the number of reacting terminal groups) is 2.0. The sample contains NaCl as an impurity in an unknown, extremely small amount that persists after the commercial purification treatment has been carried out following the synthesis from epichlorohydrin. There may also be minute amounts of unreacted epichlorohydrin and related organic molecules as impurities, and some moisture, but their concentrations are not known. These impurities, including any hydroxyl groups, may cause errors in the assessment of the number of covalent bonds formed, but these errors are not

likely to exceed 2–3%, which is comparable to the size of the errors in our estimate of the number of covalent bonds formed from thermal measurements. Both chemicals were used on this understanding. Accurately weighed amounts of the two components were mechanically mixed inside a glass container for 2–3 minutes at 298 K, and immediately transferred to the dielectric cell of the measurement assembly. Homogeneous, transparent liquids were thus obtained.

The chemical reactions between the amine and the diepoxide are addition reactions, with no other product except one, larger molecule. The cyclic, terminal epoxide group opens, and its oxygen atom accepts a proton from the amine's NH_2 group to form an –OH group, and the terminal carbon atom forms a covalent bond with the N atom of the amine. This leads to a linkage between one end of the diepoxide molecule and the primary amine, which becomes a secondary amine, e.g., R′–CH(OH)–CH_2–N(C_6H_{11})H, where R′ denotes the remaining part of the DGEBA molecule which contains the second terminal epoxide group, and C_6H_{11} denotes the cyclohexyl group. The proton of the secondary amine is accepted by the oxygen atom of the epoxide group of another diepoxide molecule, which bonds with the N atom, producing R′–CH(OH)–CH_2–N(C_6H_{11})–CH_2–CH(OH)–R′. The next reaction of a second amine molecule is with the epoxide contained in the R′ group. The process ultimately produces mainly a linear chain structure, with C_6H_{11} groups as pendants to a chain of the type –A–B–A–B–, where A is the [–CH_2–CH(OH)–(bisphenol)–CH(OH)–CH_2–] group of the DGEBA molecule and B the [–N(C_6H_{11})–] group of the cyclohexylamine molecule.

The calorimetric data were needed to calculate the number of covalent bonds formed during the course of polymerization of a liquid, and, for the sake of accuracy, it was also important that these data and the dielectric spectra be obtained for the same sample. This was done continuously over time, and almost simultaneously, either at a constant temperature or at temperatures decreasing or increasing at a controlled rate, by means of an instrument designed for the purpose and referred to here as the simultaneous impedance and thermal analyser (SITA). It was used here to measure at any instant and in a continuous-time manner two properties: (i) the dielectric permittivity and loss spectra, and (ii) the rate of heat evolution or absorption in a physical or chemical process. The spectra are measured over the frequency range 45 Hz to 0.5 MHz, and the time taken to collect the capacitance and conductance data in this range is 70 s. Briefly, SITA consists of a concentric electrode assembly of nominal geometric capacitance 14 pF, which is filled with the liquid at room temperature. The assembly is then inserted in a thermal bath maintained at a desired temperature. The temperature of this bath can be changed at a controlled rate. The electrical impedance measurement part of SITA was built by computer interfacing a Precision RLC Meter, Model 7400, manufactured by Quadtech of the GenRad Corporation. The heat evolved as a result of the polymerization reaction is measured simultaneously by means of a calorimetric cell into which the dielectric cell is inserted. The calorimetric cell is based on a design published before [21]. The total volume of the liquid required for the experiment is 1 ml. The stray capacitance of the dielectric cell is zero or negligible.

Before beginning the measurements on a polymerizing liquid, both the dielectric and calorimetric parts of SITA were calibrated for the capacitance and conductance, and the heat and temperature measurements. Data were obtained for the empty cell, and these data served as a base-line for the processing of the data on the liquid or solid sample. Although the temperature during the measurement period, which was as long as 24 h in some cases, was controlled to within 20 mK, the heat evolved during the polymerization reaction caused the temperature to rise. This rise was maximum when the polymerization

rate was highest, and was by at most 0.2 K. Thus the measurements reported here during the course of polymerization varied within ±0.1 K of the reported temperature. For all of the other measurements, this variation was within 20 mK.

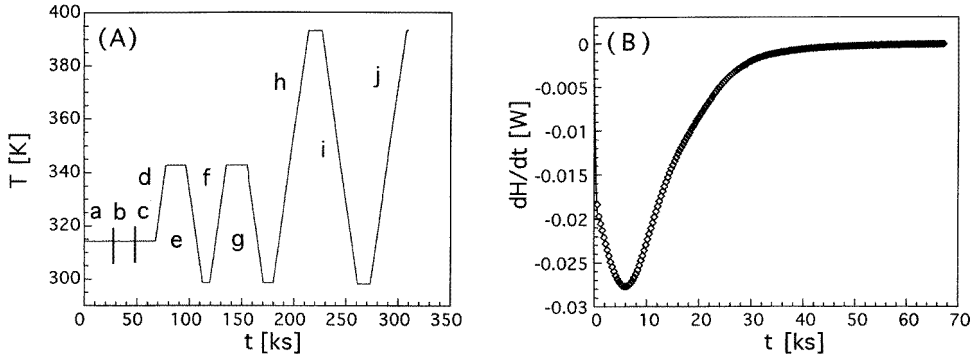

Figure 1. (A) The time–temperature conditions during the course of the dielectric and heat measurements. (B) The rate of heat release during the polymerization of the cyclohexylamine–DGEBA mixture is plotted against the time for which the polymerization has been proceeding, at 314.2 K. The regions identified as a, b, c, etc, refer to the regions in which the data are shown in subsequent figures.

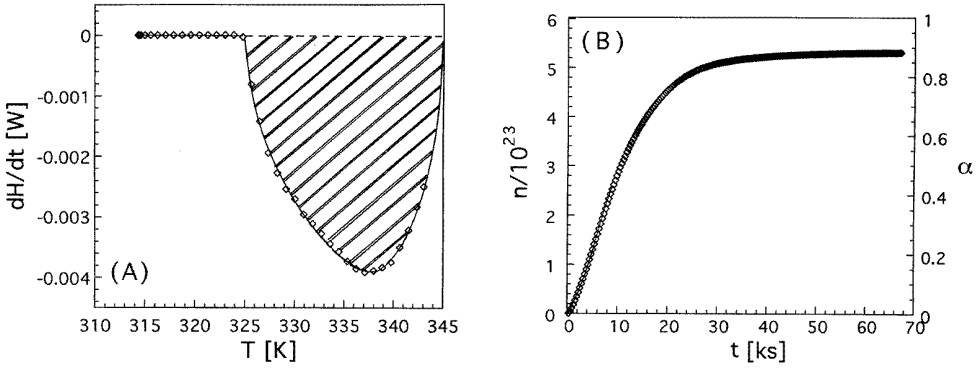

Figure 2. (A) The rate of heat release during the polymerization on heating from 314.2 K to 331.5 K at the rate of 10 K h^{-1} is plotted against the temperature. (B) The number of covalent bonds formed, n, and the extent of the reaction, α (right-hand scale), are plotted against the time for which the reaction has been proceeding. These values were calculated from the data shown in figure 1 and figure 2(A).

3. Results

The conditions of temperature and time for which the polymerization of the equimolar cyclohexylamine–DGEBA mixture was carried out, and studied by dielectric spectroscopy and calorimetry, are shown in figure 1(A). The mixture was kept isothermally at 314.2 K for 18.7 h (67.2 ks) during which both the rate of heat evolvement, $(\mathrm{d}H/\mathrm{d}t)_T$, as a result of covalent bond formations, and the dielectric spectra were measured. Figure 1(B) shows the rate of heat evolvement as a function of time. After isothermal polymerization for 18.7 h,

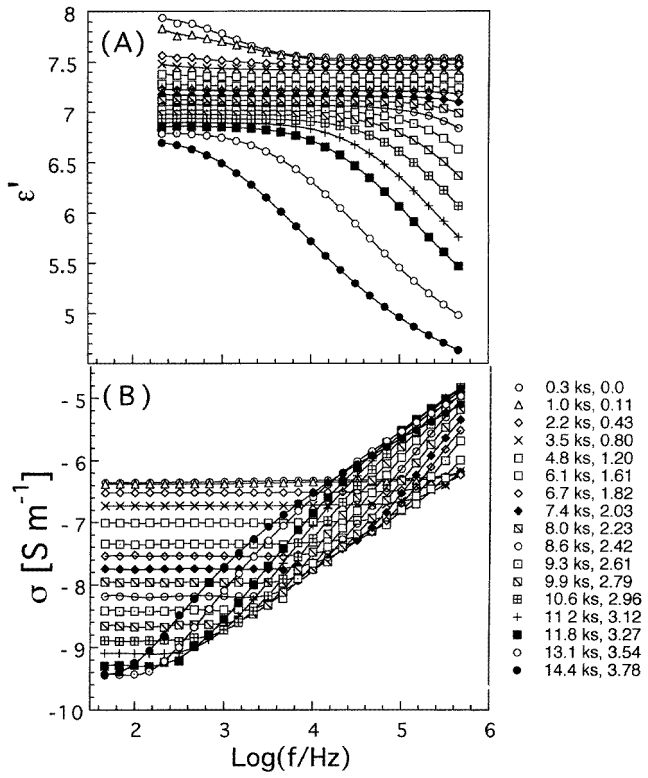

Figure 3. The dielectric permittivity and the conductivity spectra for different states of polymerization of the cyclohexylamine–DGEBA mixture at 314.2 K containing different numbers of covalent bonds. The notation refers to the number of bonds, n, divided by 10^{23}, as indicated. The region covered is part a in figure 1(A).

the sample was heated to 341.5 K at the rate $q = 10$ K h^{-1}, during which the heat evolved $(\mathrm{d}H/\mathrm{d}t)_q$, was continuously measured as a function of temperature. These data are plotted in figure 2(A). The total heat evolved is equal to the integrated area of the curve in figure 1(B) and that in figure 2(B) plus all other heat evolved during repeated heating to 341.5 K and to 394 K, and isothermally maintaining these two temperatures. This total heat, ΔH^0, is the heat of reaction for the 314.2–394 K range. On the assumption that ΔH^0, which is 111 kJ per mole of the total molecular content of the mixture, is almost independent of the temperature in this range, the extent of the reaction, α, was calculated. It is numerically equal to the heat evolved at a time t, as determined from the integrated area up to time t divided by ΔH^0. This quantity was determined for polymerization at 314.2 K, i.e., over the first isothermal region of 18.7 h in figure 1(A), and is plotted against t, the duration of the reaction, in figure 2(B).

To convert these data into the number of bonds formed, n, we proceeded as follows: since one cyclohexylamine molecule forms two covalent bonds with two DGEBA molecules, one of which in turns forms two covalent bonds with two cyclohexylamine molecules, a linear chain structure of the type –A–B–A–B–, with cyclohexyl groups as pendants to the chain, is formed. This chain grows on further reaction. On the assumption that the number of oligomers formed is small or negligible, the total number of covalent bonds formed in this case will be equal to the total number of molecules present initially, i.e. the Avogadro

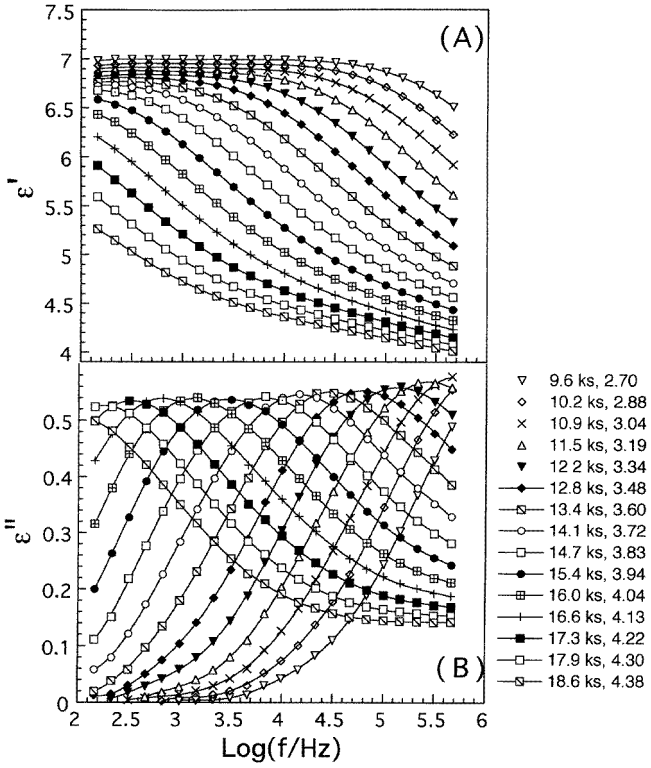

Figure 4. The permittivity and loss spectra obtained during the course of polymerization of the cyclohexylamine–DGEBA mixture at 314.2 K are shown for different numbers of bonds formed. The notation refers to the number of bonds, n, divided by 10^{23}, as indicated. The spectra show the shift of the α-relaxation process towards a lower frequency as the number of bonds increased. The region covered is part b in figure 1(A).

number, N_A, per mole of the total molecular content of the mixture. Thus the heat evolved per covalent bond formation is equal to $\Delta H^0/N_A$ which is 18.4×10^{-20} J/bond. This leads to $n = \alpha N_A$, which is also plotted against t in figure 2(B). The sigmoid-shaped curve thus obtained was then used to convert t into n, so the equilibrium dielectric behaviour and the dynamics of dipolar diffusion may be discussed in terms of a liquid structural property, n, and not the duration of the reaction.

For the convenience of the discussion, the total period of isothermal polymerization at 314.2 K has been divided into three regions: a, b, and c, as shown in figure 1(A), because different aspects of the dielectric properties and of their changes become evident, and even dominate in these regions. The permittivity, ε', and conductivity, σ, spectra for the first region, a, are shown in figure 3. The plot for the lowest n shows a small step decrease in ε', as well as a rise toward a plateau-like feature in σ. In this region, the interfacial polarization seems to contribute significantly to both ε' and σ in the early period of polymerization. After about 1 ks ($n = 0.5 \times 10^{23}$), this contribution vanishes, and only the low-frequency, plateau-like features of ε' and σ are observed. These correspond to the static permittivity, ε_s, and the dc conductivity, σ_0. As polymerization continues, and n increases, both ε' and σ show dependence on the frequency, ε' decreasing towards a limiting value and σ increasing towards its limiting value before reaching the corresponding infrared

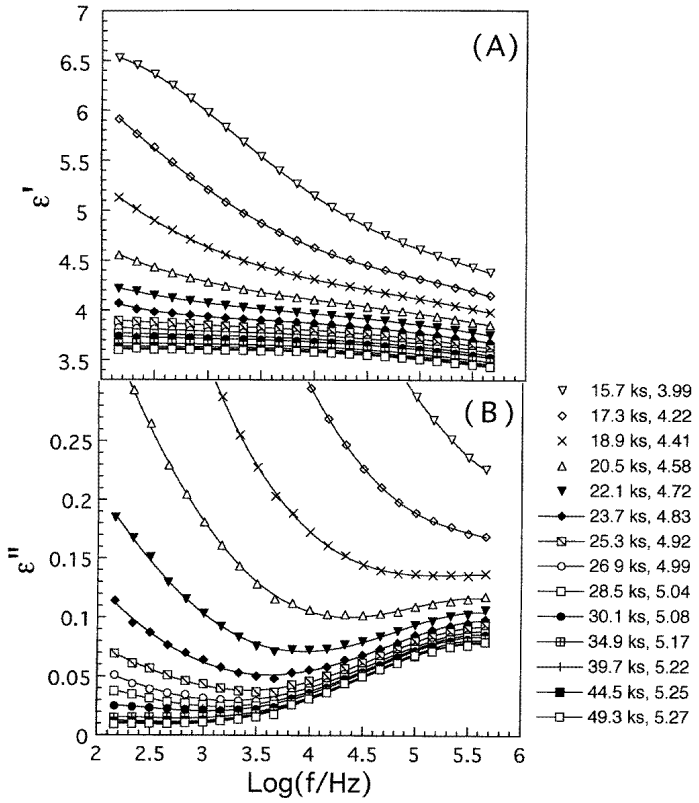

Figure 5. The permittivity and loss spectra obtained during the course of polymerization of the cyclohexylamine–DGEBA mixture at 314.2 K are shown for different numbers of bonds formed. The notation refers to the number of bonds, n, divided by 10^{23}, as indicated. The spectra show the evolution of a new relaxation process at higher frequencies. The region covered is part c in figure 1(A).

permittivity and conductivity values. These effects are remarkably similar to those observed when a chemically stable liquid or solid is cooled.

The dielectric permittivity, ε', and loss, ε'', spectra obtained for the conditions in region b of figure 1 are shown in figure 4. These show clearly an ε''-peak, which shifts towards the low-frequency side as n increases on polymerization irreversibly, in a manner remarkably similar to that observed for a liquid or a solid on cooling. The ε'- and ε''-spectra for the conditions in region c of figure 1 are shown in figure 5. Here the peak has moved out of the frequency range, and a new relaxation process becomes evident, i.e. ε' shows a small, new dispersion and ε'' an approach towards a peak value. The high-frequency part of this peak cannot be discerned even when n has increased from 4.7×10^{23} to 5.3×10^{23}. This is partly due to the decrease in the height of the peak itself, but mainly due to the insensitivity of this relaxation process to increase in n, as recently observed from measurements at GHz frequencies, and discussed elsewhere [22].

The ε'- and ε''-spectra measured during the course of heating from 314.2 to 341.5 K at 10 K h^{-1} are shown in figure 6. As T increases in this experiment, the polymerization becomes faster, and n increases initially at a faster rate. These spectra, for which T and n are given in figure 6, show that starting from 314.3 K, an increase in T and n causes ε''

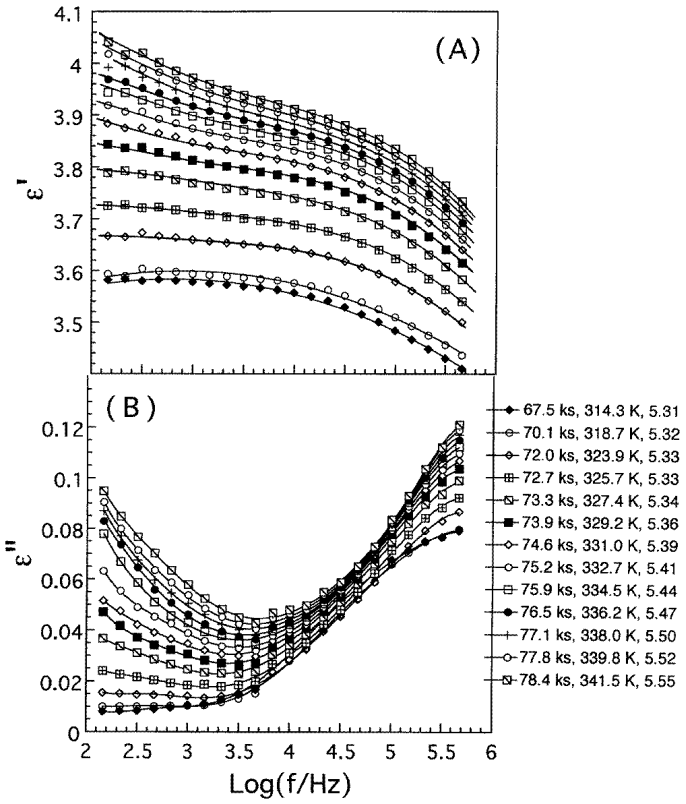

Figure 6. The permittivity and loss spectra obtained during the course of heating from 314.2 to 331.5 K at 10 K h^{-1} are shown for selected temperatures and values of n, the number of covalent bonds formed at the instant at which the spectra were obtained. It is divided by 10^{23}. The region covered is part d in figure 1(A).

to decrease first and then to increase, and ε' to increase. The initial decrease is a reflection of the shift of the low-frequency relaxation peak towards still lower frequencies, and the increase is a reflection of the shift of this peak towards higher frequencies, although the peak has not appeared in the spectral range of figure 6. This, as will be discussed later here, is a consequence of compensatory effects of the increase in n, that decreases the rate of relaxation, and the increase in T, that increases it.

4. Discussion

The general pattern of the evolution of the molecular dynamics during the course of macromolecular growth as a result of polymerization, as observed here, is remarkably similar to that observed for liquids and solids during isobaric cooling or during isothermal compression. There are also of course several other aspects in which the equilibrium and dynamic behaviours differ from those observed on cooling and compression, which need to be discussed. For this purpose we begin the discussion of each aspect at first isolated from the others, and then we combine them into a general picture that emerges from this study.

4.1. The interfacial polarization and the dc conductivity

It is well recognized that the dielectric permittivity, ε', and loss, ε'', of a material, as measured in a dielectric cell, are the sums of four effects generally: the interfacial polarization, the dc conductivity, the orientational polarization, and the vibrational and the optical polarizations [23–26]:

$$\varepsilon' = \varepsilon'_{int} + \varepsilon'_{dip} + \varepsilon_\infty \tag{1}$$

$$\varepsilon'' = \varepsilon''_{dc} - \varepsilon''_{int} + \varepsilon''_{dip} \tag{2}$$

where

$$\varepsilon'_{int} = Z_0 \sin(m\pi/2)[\{(\sigma_{dc} + \sigma_{dip})^2 C_0\}/\varepsilon_0^2]\omega^{-(m+1)} \tag{3}$$

and

$$\varepsilon''_{int} = Z_0 \cos(m\pi/2)[\{(\sigma_{dc} + \sigma_{dip})^2 C_0\}/\varepsilon_0^2]\omega^{-(m+1)} \tag{4}$$

where Z_0 and m are characteristics of the electrode/material interface in the ε'- and ε''-equations for complex impedance, $Z^*_{el} = Z_0(\mathrm{i}\omega)^{-m}$, C_0 refers to the geometric capacitance of the empty dielectric cell, and ω refers to the angular frequency ($\omega = 2\pi f$ (Hz)). ε_0 is the permittivity of vacuum (8.8514 pF m^{-1}). Cole and co-workers [23, 24] have found that $m = 0.5$, which corresponds to the Warburg impedance. The measured conductivity is

$$\sigma = \sigma_{dc} + \sigma_{int} + \sigma_{dip} \tag{5}$$

where

$$\sigma_{int} = Z_0[\cos(m\pi/2)]\{(\sigma_{dc} + \sigma_{dip})^2 C_0/\varepsilon_0\}\omega^m. \tag{6}$$

According to equations (3)–(6), the interfacial contribution is largest for the lowest value of ω of one's measurements, where σ_{dip} approaches zero, and decreases rapidly as ω is increased. For a fixed ω it is also large when σ_{dc} is large. We analyse the low-frequency data in the spectrum for $n = 0$ to 0.11×10^{23}, in the same manner as before [26], and obtain the values $Z_0 = 0.265$ MΩ m^{-1}, and $m = 0.5$. By deducting the interfacial contribution from the measured values of both σ and ε' for the conditions where $0 < n < 1.2 \times 10^{23}$, we obtain ε_s and σ_{dc}. For n between 1.2×10^{23} and 3.78×10^{23}, ε_s and σ_{dc} are readily obtained from the plateau values of the curves, as is seen from the spectra in figure 3.

For $n > 3.78 \times 10^{23}$, σ_{dc} was determined from an analysis of the ε''-data for the low-frequency part of the spectrum. This was done by subtracting an estimated magnitude of σ, which did not give negative values of ε'' at any frequency of the spectra, and the remaining value of ε'' consistently increased from the lowest ω towards the peak value. This estimate of σ was taken as equal to σ_{dc}. All of the values of σ_{dc} determined in this manner are plotted against t and n in figure 7.

It should be noted that these are the first set of studies in which σ_{dc} has been determined appropriately from the dielectric spectra. For determining σ_{dc} in all earlier studies [1, 6, 27], the electrical modulus formalism was used, with the reasonable approximation that dc conduction involves a single Maxwell relaxation time. Furthermore, the procedure used in the earlier studies also failed to yield an accurate value of σ_{dc} at small n, where the contribution to σ from interfacial polarization is significant, and at large n, where the contribution to σ from dipolar reorientation becomes significant. With the more accurate data available now, it seems pertinent to discuss the reasons for the decrease in σ_{dc} with the increase in t and n. The equations with which we attempted to fit the data are [1, 27, 28]

$$\sigma_{dc} = A_\sigma \exp[B_\sigma/(t_0 - t)] \tag{7}$$

$$\sigma_{dc} = \sigma_{dc}(n = 0)[(n_x - n)/n_x]^p \tag{8}$$

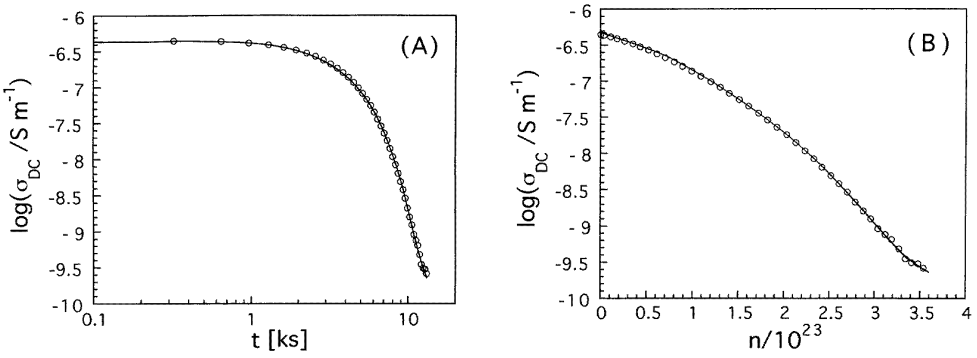

Figure 7. The dc conductivity determined from the data in figure 3 is plotted against (A) the time for which the polymerization reaction has been proceeding, and (B) the number of covalent bonds formed during the polymerization.

where t_0 and n_x are the respective values of t and n at which σ_{dc} formally approaches zero, and p is an empirical parameter. Neither of the above two equations was found to fit the data satisfactorily, which shows that the mechanism by which σ_{dc} decreases with t and n for the growth of linear chain macromolecules differs fundamentally from the mechanism by which it decreases for the growth of a network macromolecule.

It is conceivable that the linear chains formed on polymerization become long enough to entangle, and that the number of such entanglements becomes high enough to lead to the formation of a gelled structure, as is for example the case for ordinary water-based gelatin gel. But the dc conductivity in this mechanism does not change significantly after the gelatin sol has become a gel. Here the bond percolation concept [29] is not applicable in the same manner as for the cross-linking polymerization, where the gelation time could be determined [1, 6, 27, 28].

One of the more significant aspects of the study which is evident in figure 7(B), but which was not observed before, is the somewhat inverted sigmoid shape of the plot of σ_{dc} against n. This shape implies that there is a single underlying mechanism according to which σ_{dc} changes, such that the rate of change is maximum at a certain value of n, and thereafter σ_{dc} reaches its limiting value as $n \to N_A$. This mechanism is likely to be the one that is dominated by the translational diffusion of ions formed on ionization of NaCl, H_2O, and other impurities whose population decreases towards a limiting value as a result of the decrease in the equilibrium permittivity, ε_s, towards a limiting value, according to the equation for the ion $\leftrightarrow$ ion-pair equilibria [33]:

$$K_A = \left(\frac{C_{\text{ion-pair}}}{C_{\text{cation}}C_{\text{anion}}}\right) = \frac{4\pi N_A^3}{3000}\exp\left[\frac{z_1 z_2 e^2}{a\varepsilon_s k_B T}\right] \tag{9}$$

where C refers to the concentration of the entity written as the subscript, K_A is the ion-pair association constant, N_A the Avogadro number, z_1 and z_2 the electronic charges on the ions, e the magnitude of the electronic charge, a the ion-size parameter, and k_B the Boltzmann constant.

Alternatively, the shape of the plot of σ_{dc} against n in figure 7(B) can be seen as a consequence of at least two sets of effects, namely:

(I) a decrease in σ_{dc} when:

(i) the charge carrier's mobility (that of Na^+, Cl^-, H^+, OH^-, or other impurity ions) decreases with the increase in the viscosity as n increases; and

(ii) the populations of the same ions decrease as ε_s decreases with the increase in n; and

(iii) any H-bonded network structure through which the amine protons can translocate is gradually depleted; and

(II) an increase in σ_{dc} from zero towards a limiting value at $n \rightarrow N_A$ as a new H-bond network structure involving the –OH groups forms on reaction, and thereby a new path for translocation of protons develops with the increase in n.

The last effect requires a near-neighbour H-bond formation leading to the connection of molecules by H bonds. Evidence for the formation of H bonds in the reactive epoxy–amine mixture has been obtained by near-ir spectroscopy studies [34], since the suggestion was made that the conduction mechanism may also be partly due to the proton translocation through the near neighbours [35]. Thus mechanism (II) is supported by experiments.

It seems that the decrease of σ_{dc} involves both the decrease in the populations of impurity ions as charge-carrying entities, and translocation of protons along the H bonds towards a limiting value as ε_s approaches a limiting value on polymerization, and the compensatory effects of I and II. Equations for the approach of σ_{dc} towards a singularity according to the bond-percolation theory [28] for gel formation are not relevant here because a cross-linked structure does not form on polymerization. It is noteworthy that the limited data on σ_{dc} available in the earlier studies [1, 2, 6, 27, 31, 33] had masked this compensatory effect.

4.2. The equilibrium polarization and polymerization

The equilibrium dielectric permittivity, ε_s, which corresponds to the sum of all of the molecular polarizations, is plotted against n in figure 8. It decreases with increase in n, according to the equation

$$\varepsilon_s = 6.53 + 1.09/[1 + \exp\{(n/10^{23}) - 2.3\}] \tag{10}$$

which gives an inverse sigmoid shape for the plot of ε_s against n. As the molecular mixture polymerizes, ε_s changes for several reasons, namely:

(i) the mixture's density increases;

(ii) certain dipoles associated with the epoxide and amine groups vanish, and others such as those associated with the –OH and $–CH_2–N(C_6H_{11})–CH_2–$ form;

(iii) the dipolar orientational correlation factor changes, as the dipolar alignment of the linear chains becomes distributed differently, and chains fold on themselves, and possibly entangle with each other such that the interchain interactions change; and

(iv) the limiting high-frequency permittivity, ε_∞, changes, because both the optical refractive index and the infrared polarization change.

So, it is remarkable that the net effect observed here is that ε_s decreases, because densification of the liquid alone would be expected to raise it. A polymer's density of course increases as its molecular weight or n increases, and in some cases the values of ε_s are also found to decrease—as for example, ε_s for propylene glycol decreases from about 50 to about 5 when it is polymerized to poly(propylene glycol), of average molecular weight 4000 [36]. Rationalization of such a decrease in terms of the consumption of some dipoles and production of others has been difficult in chemical terms, mainly because of the multiplicity of the dipolar groups and molecules that exist during the course of polymerization. Nevertheless, such observations are rationalized in general physical terms in molecular dielectric theories, as follows.

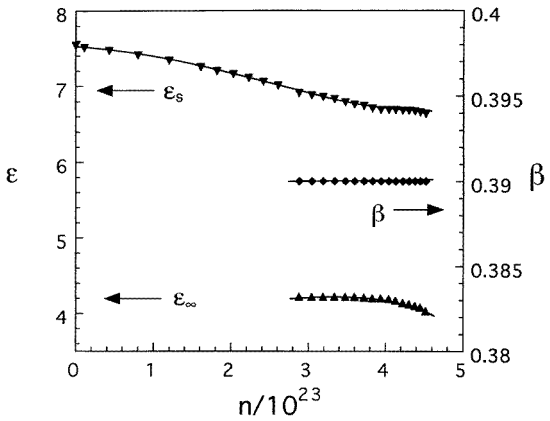

Figure 8. ε_s, ε_∞, and β are plotted against the number of bonds formed during the polymerization reaction at 314.2 K.

Strictly interpreted in terms of the formalism of statistical dielectrics theory developed by Onsager [37], Kirkwood [38], and Fröhlich [39],

$$\varepsilon_s = \varepsilon_\infty + \left[\left(\frac{\varepsilon_\infty + 2}{3}\right)^2 \left(\frac{\varepsilon_s}{2\varepsilon + \varepsilon_\infty}\right)\right] \frac{4\pi N_d g \mu_0^2}{k_B T} \tag{11}$$

where N_d is the number density of the dipoles, g is the dipolar orientational correlation factor, as defined by Kirkwood, μ_0 is the vapour-phase dipole moment, and all other terms have the same meaning as before. According to equation (11), a decrease in ε_s at constant T means that $g\mu_0^2$ decreases on polymerization, or that the increase in both ε_s and in ε_∞ due to an increase in N_d is dominated by the decrease in $g\mu_0^2$ as n increases on polymerization.

The rate of decrease in ε_s with increase in n, i.e., the magnitude of $(\mathrm{d}\varepsilon_s/\mathrm{d}n)_T$, as determined from figure 8, varies with n itself, and the curve has an inverted sigmoid shape. Its maximum value is -1.1 per Avogadro number of bonds formed. The rate of this decrease is obtained by differentiating equation (11):

$$\frac{\partial \varepsilon_s}{\partial n} = \frac{\partial \varepsilon_\infty}{\partial n} + y\mu_0\left(\frac{\partial N_d}{\partial n} g\mu_0 + \frac{\partial g}{\partial n} N_d \mu_0 + \frac{\partial \mu_0}{\partial n} 2N_d g\right) + \frac{\partial y}{\partial n} \frac{4\pi N_d g \mu_0^2}{k_B T} \tag{12}$$

where y represents the entire term enclosed in the square brackets in equation (11). The limiting high frequency of all orientation polarizations (i.e., including that of the faster process after it has separated), ε_∞, is also plotted against n in figure 8. It too decreases with increase in n. From its maximum slope, we obtain that $\mathrm{d}\varepsilon_\infty/\mathrm{d}n$ is equal to -0.2 per mole of bonds formed. Since the volume decreases at most by 10–15%, the term $\mathrm{d}N_d/\mathrm{d}n$ in equation (12) is expected to be about 0.11molecules per molar volume per Avogadro number of bonds formed. It is not known whether the overall value of μ_0 of the polymer chain here is greater than the average weighted sum of the values of μ_0 of the original monomer molecules in the liquid, but in most cases $\mathrm{d}\mu_0/\mathrm{d}n$ decreases on polymerization. The first two terms in the large brackets in equation (12) are negligibly small for the magnitudes of ε_s and ε_∞ observed in figure 8, and the last term in these brackets is negative. Hence, as $\mathrm{d}N_d/\mathrm{d}n$ is positive, $\mathrm{d}\mu_0/\mathrm{d}n$ is expected to be negative. So, either $\mathrm{d}g/\mathrm{d}n$ is also negative, or it is positive with a magnitude such that the absolute value of the sum of the $(\mathrm{d}N_d/\mathrm{d}n)g\mu_0$ and $(\mathrm{d}g/\mathrm{d}n)N_d g$ terms is less than that of the $(\mathrm{d}\mu_0/\mathrm{d}n)2N_d g$ term in

equation (12). Resolution of these terms is possible by means of further experiments on the dipole moment of the partially polymerized states of the initially monomeric liquid.

The decrease of ε_α on increase in n (densification), as seen in figure 8, is also remarkable, because it is expected to increase on densification as the optical refractive index increases according to the Lorenz–Lorentz equation. This increase was expected only when $\Delta\varepsilon_{vib}$, the contribution to the polarization from the vibrational polarization, remained constant, and Johari–Goldstein relaxations were absent at higher frequencies. It is generally recognized that densification raises the frequency of the vibrational modes, and since $\Delta\varepsilon_{vib}$ is directly proportional to the integrated absorptivity of that mode and the inverse square of its frequency, it follows that the increase in the vibrational frequencies on densification will lower $\Delta\varepsilon_{vib}$, provided that any increase in the absorptivity is small and that there is no contribution from the Johari–Goldstein relaxation. A resolution of these contributions requires a study in the future of the refractive index, far-ir spectra, and the GHz frequency spectra during the course of polymerization.

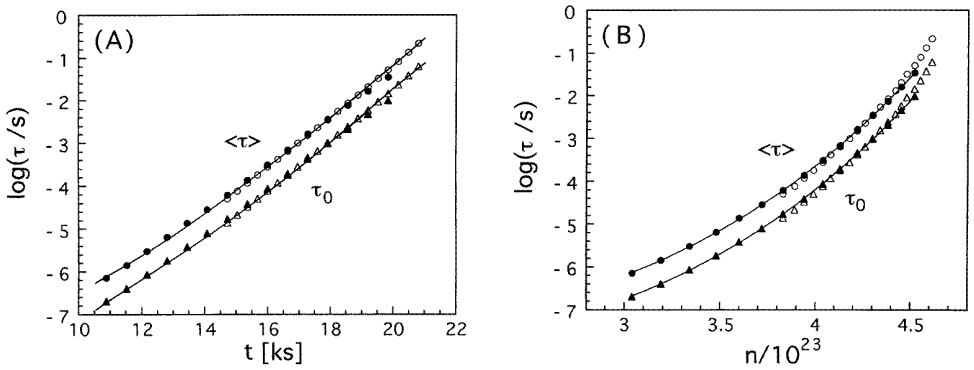

Figure 9. The characteristic and average relaxation times of the liquid in the various states of its polymerization are plotted against (A) time, and (B) the number of covalent bonds formed. Circles represent the values calculated from the data obtained with the frequency fixed at 1 kHz using the earlier-described procedure of Johari [1].

4.3. The relaxation time and its distribution

As is done generally for determining the relaxation time and its distribution, we use the normalized relaxation function, $\Phi = \exp[-(t'/\tau_0)^\beta]$, as originally given by Debye for $\beta = 1$, or a single relaxation time. Here t' refers to the period of observation for a dipolar relaxation, t_0 is the characteristic relaxation time, and β is now known as the stretched exponential parameter; its value, between 0 and 1, is a measure of the broadness of the distribution of relaxation times. The mean relaxation time is $\langle\tau\rangle = (\tau_0/\beta)\Gamma(1/\beta)$, where Γ refers to the gamma function. The permittivity and loss spectra obtained for different values of n shown in figure 4 were analysed in terms of this relaxation function, and the values of β and τ_0 were determined. The values of β and $\langle\tau\rangle$ calculated from τ_0 are plotted against n in figures 8 and 9(A), respectively, and $\langle\tau\rangle$ is also plotted against logarithmic t in figure 9(B).

Over the range $2.3 \times 10^{23} < n < 4.4 \times 10^{23}$, β remains constant at 0.39 ± 0.01, as is seen in figure 8. But for lower values of n, it is likely to be higher, and to have a decreasing value [14]. Since, for $n = 0$, there is only one relaxation process in the GHz

frequency range, for which β is considerably more than 0.4 [22], and the α-relaxation has not yet separated from the Johari–Goldstein relaxation in the low-viscosity, liquid state, it seems inappropriate to compare the values of β for the GHz frequency relaxation with that observed here. It is worth noting that the value of β of 0.39 observed here is much less than that for other polymers and glass-forming liquids, but is comparable to that for polymers formed with diglycidyl ether of bisphenol-A (DGEBA) which is also used here, irrespective of whether a linear chain structure or a network structure is formed. It appears that a low value of β, or equivalently a broader distribution of relaxation times found generally in the DGEBA-containing polymers, is a reflection of the large, repeat units in the polymer's structure. A survey of the earlier studies showed that when the repeat unit in a polymer is relatively small, as for example it is in poly(vinyl chloride) and poly(methyl methacrylates), the distribution is relatively small, β is higher than 0.5, and the dielectric spectra are relatively narrow [40]. In contrast, for proteins and DNA, where the repeat units are relatively large, β becomes much less, and the spectrum of relaxation times becomes extremely broad [41–43].

We now consider the increase in the characteristic relaxation time, τ_0, during the macromolecular growth as a result of polymerization. As is seen in figure 9, τ_0 increases with increase in n as well as with increase in t. But the manner in which it increases with increase in n differs from the manner in which it increases with increase in t. This is obviously due to the fact that n and t are not related linearly, as is evident from figure 2(B). Nevertheless, a remarkable difference between the shapes of the two plots in figure 9(A) and 9(B) is expected on the basis of two observations:

(i) n increases with t according to a sigmoid-shaped curve, as seen in figure 2(B); and

(ii) since t continues to increase naturally, even when n and τ_0 have reached their limiting values, measurements extended beyond the value of t when τ_0 has reached a limiting value will yield a horizontal curve of τ_0 against t at long times. This will distort the plot of τ_0 against t to produce a sigmoid shape, but not the plot of τ_0 against n.

In our earlier studies [15, 31, 32], a relation between τ_0 and the extent of the reaction α was found to describe the relaxation dynamics during polymerization:

$$\tau_0 = \tau_0(\alpha = 0)\exp[S\alpha^p] \tag{13}$$

or

$$\tau_0 = \tau_0(n = 0)\exp[S(n/N_A)^p] \tag{14}$$

where S is equal to the normalized value of τ_0 at the polymerization temperature, i.e., $S = \ln[\tau_0(n = N_A)/\tau_0(n = 0)]$, and p is an empirical parameter, characteristic of a polymerization reaction. Although τ_0-values for $n < 2.3 \times 10^{23}$ are not available here, equation (14) may still be fitted to the τ_0-data. This yields $\tau_0(n = 0) = 6.7$ ns, $p = 3.57$, and $S = 169.8 \times 10^{20}$. The curve calculated from these parameters is shown in figure 9, which confirms our earlier finding that a relationship between τ_0 and n can be written in the form of equations (13) and (14). The quantity S is of course a material parameter, and is temperature dependent. A comparison of the p-values for various polymerization reactions shows that its value is also a characteristic of the polymerizing material.

There is one more issue that deserves further examination. In their earlier studies, Johari and co-workers [1, 6, 27] have determined the relaxation time, τ_0, by analysing the permittivity and loss data that they had measured for a single fixed frequency, usually 1 kHz, during the course of isothermal polymerization. For convenience, they simplified the normalized relaxation function, $\Phi = \exp[-(t'/\tau_0)^\beta]$, to $\Phi(t) = \exp[-(t'/\tau_0(t))^{\beta(t')}]$, or

equivalently, $\Phi(n) = \exp[-(t/\tau_0(n))^{\beta(n)}]$, where Φ and β also vary with t and n. On the assumption that b, ε_s, and ε_∞ are much less sensitive to t and n than τ_0, and to simplify the calculations and reduce the number of experiments needed to determine τ_0 from the dielectric spectra, they replaced $\beta(t)$ or $\beta(n)$ by a fixed, t- and n-independent, parameter γ, and called it the reaction parameter. Their procedure has been criticized recently [44], and an objection raised to its use.

To examine the validity of the procedure of Johari and co-workers [1, 6, 27], and the merits of the recent objection [44] to its use for obtaining τ_0 during the growth of a macromolecule, we analysed our data by means of their procedure. For this purpose we used the ε'- and ε''-data only for one fixed frequency, 1 kHz. This analysis gave $\gamma = 0.35 \pm 0.01$, and a set of τ_0-values for different n, which are shown by circles in figure 9. Evidently, their procedure yields a value for γ equal to that of β, as determined from the exact procedure using the spectra here. It also gives the same values for τ_0 at different n, within the experimental errors. We conclude that the criticism of the procedure of Johari and co-workers, which uses measurements for a single, fixed frequency, remains unjustified, as has been concluded by several other workers [13, 15, 16, 30] from experiments and from calculations [45]. It must, however, be stressed again that a Fourier transform of the Debye relaxation function into the approximate equation that Johari and co-workers used is not possible. Although the two procedures yield the same distribution parameter and τ_0, within experimental error, the two equations used in the procedure do not commute, as has been pointed out before [1, 5, 18, 27].

4.4. Configurational entropy and polymerization

As polymerization occurs, the viscosity increases, the diffusion coefficient decreases, and the configurational entropy of the system decreases. The absolute configurational entropy is related to the relaxation time according to the Adam–Gibbs formalism [46]:

$$\tau(T) = \tau(T \to \infty) \exp\left(\frac{\Delta\mu\, s_c^*}{S_{conf} k_B T}\right) \tag{15}$$

where $\Delta\mu$ is the potential energy hindering the cooperative rearrangement of the molecule per repeat unit or monomer, s_c^* is the critical entropy, S_{conf} is the configurational entropy, and k_B is the Boltzmann constant. $\tau(T \to \infty)$ is the relaxation time when $TS_{conf} = \infty$. In their interpretation of various polymeric and nonpolymeric liquid relaxations, Adam and Gibbs noted that $\Delta\mu\, s_c^*$ is a constant for a material. We assume therefore that $\Delta\mu\, s_c^*$ remains constant as the size of the macromolecule grows on polymerization, or that $\Delta\mu\, s_c^*$ is independent of n. Thus equations (14) and (15) may be combined to obtain

$$S_{conf} = \Delta\mu\, s_c^* \Big/ \left[\left[k_B T \left\{\ln\left[\frac{\tau(n=0,T)}{\tau(T \to \infty, n)} + S(T)\left(\frac{n}{N_A}\right)^p\right]\right\}\right]\right] \tag{16}$$

where $\tau_0(n = 0, T)$ is the value for $n = 0$ at the given temperature T, and $\tau_0(T \to \infty, n)$ is the value as $T \to \infty$ for a given value of n. S and p are as defined earlier, and it is assumed that $\Delta\mu\, s_c^*$ does not change on polymerization. When T is constant, the two terms within the square brackets in equation (16) increase during the course of polymerization, and when n is constant these same two terms change implicitly with explicit change in T. Thus it seems possible to find conditions for which an increase in n on polymerization can bring the material's structural state to the same value of t_0 to which a decrease in T of a different (chemical) structural state of the material with the same components will bring it. Thus a decrease in n at a certain temperature becomes equivalent to a decrease in $k_B T$

in terms of the molecular kinetics, not of the structure. Superficially, this seems to have a parallel in the effect of pressure, where the same value of τ_0 can be achieved under a variety of conditions of T and pressure, but without a change in the chemical structure. It also needs to be recalled that the achieving of the same τ_0-value here involves the loss of predominance of the van der Waals interaction to the directionally restricted interaction of covalent bonds.

The conditions for which τ_0 can be brought to the same value by using different procedures can be obtained by differentiating equation (14):

$$(\mathrm{d}\ln\tau_0/\mathrm{d}n)_T = SpN^{p-1} \tag{17}$$

in which the change in τ_0 with n is irreversible, i.e., $(\mathrm{d}\ln\tau_0/\mathrm{d}n)_T$ is always positive for polymerization (it will become negative for polymer degradation), and

$$\left(\frac{\partial\ln\tau}{\partial T}\right)_n = -\Delta\mu\, s_c^* \left[T\left(\frac{\partial S_{conf}}{\partial T}\right) + S_{conf}\right] \Big/ k_B T^2 S_{conf}^2. \tag{18}$$

By combining equations (17) and (18), we obtain the equivalence between n and T, as

$$\left(\frac{\partial n}{\partial T}\right)_\tau = \frac{\Delta\mu\, s_c^*}{S_p k_B}\left[\left\{T\left(\frac{\partial S_{conf}}{\partial T}\right) + S_{conf}\right\} \Big/ \left\{T^2 S_{conf}^2 \left(\frac{n}{N_A}\right)^{p-1}\right\}\right]. \tag{19}$$

According to equation (19), this equivalence itself depends upon n, T, and S_{conf}. Experiments alone can determine these conditions, since no independent manner of determining S_{conf} is currently available.

It is significant to note that when n and T increase together, both ε' and ε'' at high frequencies increase, as is seen in the ε'- and ε''-spectra in figure 6. For example, ε'' increases from 0.08 to 0.12 at a frequency of 0.45 MHz, when n increases from 5.31×10^{23} at 314.3 K to 5.55×10^{23} at 341.5 K. A similar increase in ε'' occurs also at the low-frequency end of the spectra, from which information on the change in the relaxation rates can be deduced.

Since the spectra in figure 6 cover only the high-frequency side of the large ε''-peak of the slower dynamics relaxation process, for which the condition is that $\omega^2\tau_0^2 \gg 1$, the increase in ε'' from 0.007 to 0.095 at the lowest frequency with increase in n and T is a consequence of the ε''-peak of the slower relaxation process moving towards higher frequencies. Hence we conclude that the dynamics of the slower process and that of the new, faster relaxation process that has emerged tend to approach close to each other within their characteristic relaxation time.

4.5. The evolution of a faster relaxation process

The presence of a minima in ε'' at frequencies below 10 kHz in the spectra in figures 5 and 6 shows clearly that a new high-frequency relaxation process with a peak in the MHz region emerges, particularly as n increases from 4.5×10^{23} to 5.3×10^{23} at 314.2 K in figure 5. That such a high-frequency or faster relaxation process does exist has been established indirectly from a variety of dielectric studies [1, 15, 30, 31] and directly from the MHz-to-GHz frequency measurements [14], and from the kHz frequency measurements of its glassy, partially polymerized state at low temperatures [47]. Although only the low-frequency side of the peak of this faster relaxation is observed, it is evident that an increase in n does not provide evidence for the complete peak. This implies that the position of this relaxation peak did not change with increase in n. This is remarkable evidence for a process whose dynamics is relatively insensitive to the increase in the macroscopic viscosity or decrease in

the configurational entropy on polymerization. Such configurational-entropy-independent relaxations have been attributed to localized rotational and/or translational diffusion of molecules in the low-density and high-density defect sites in the nonhomogeneous structure of an amorphous solid, for which mathematical treatments have been possible [48].

Earlier studies [14, 15, 22, 33] have shown that before polymerization begins at a relatively high temperature, there is only one relaxation process whose ε''-peak appears in the GHz frequency range: its height rapidly decreases to a vanishingly small value on isothermal polymerization or with increase in n, but its characteristic time does not change [14, 22]. When the same molecular ($n = 0$) liquid state is cooled and vitrified, it shows an ε''-peak due to the fastest relaxation process at 143.5 K for a fixed frequency of 1 kHz, and another in the liquid state at 243.2 K [17], above its glass transition temperature, T_g. The height of the ε''-peak of the faster, low-temperature relaxation decreases and becomes vanishingly small with increase in n, but its rate does not change. With increase in n, a new relaxation peak appears in the 250 K region still in the vitrified state of the partially polymerized liquid. The height of its ε''-peak increases with increase in n, and the peak's position in a temperature plane shifts marginally towards a higher temperature. When measurements are made at a fixed temperature, such that the rates of the fastest and the intermediate relaxations are close to each other, the contribution to ε'' from the fastest relaxation continues to decrease, while that from the intermediate relaxation process increases only slowly until n has reached a certain low value, as seen in figure 2 in reference [17], with the net effect that ε'' at frequencies approaching the peak frequency decreases initially and thereafter increases. This is observed at frequencies above 10 kHz in the ε''-spectra in figures 5 and 6. Direct evidence for the ultimate increase in ε''-peak height comes from the spectra for $n = 6.02 \times 10^{23}$ shown in figure 10 (to be discussed in the next section), where the ε''-peak height of 0.13 is considerably more than that of 0.08 for $n = 5.25 \times 10^{23}$ at 314.2 K, as seen in figure 5, or 0.07 for $n = 5.3 \times 10^{23}$ at 315.6 K, as seen in figure 6. We conclude that the dynamics of the relaxation process whose peak is expected to appear in the MHz frequency range at 314.2 K in figures 5 and 6 is a combination of the two—the faster and the intermediate-rate—relaxation processes. For $n = 6.02 \times 10^{23}$, only the intermediate-rate relaxation process remains, and its peak shifts to 10 kHz on decreasing the temperature to 299.8 K, as seen in figure 10.

4.6. Dielectric changes on further polymerization

Generally speaking, polymerization processes do not reach completion under isothermal conditions, or the limiting value of n is not reached. The incompletely polymerized material needs to be heated to a higher temperature and then kept at that temperature to achieve the limiting value of n. Therefore, after the isothermal experiments at 314.2 K and heating to 341.5 K, the liquid was kept at 341.5 K for 5.3 h (19 ks), cooled to 314.2 K, and kept at that temperature for 1.8 h (6.6 ks). It was then heated back to 341.5 K, and then kept at 341.5 K for 5.5 h (19.8 ks), cooled to 314.2 K, and then kept at 314.2 K for 2.6 h (9.3 ks). Thereafter it was heated to 394 K, kept at 394 K for 3.5 h (12.7 ks), cooled to 296 K, kept at 296 K for 3.4 h (12.1 ks), and heated back to 394 K, and finally cooled to 296 K, after thermal cycling between 296 K and 394 K. In all of the segments of this thermal treatment, the heating and cooling rates were 10 K h^{-1}. The ε'- and ε''-spectra of the polymerized final state thus obtained were then measured at different temperatures, and these spectra are shown in figure 10.

A remarkable aspect of these spectra is the development of new relaxation features with increase in n. For the spectrum at 299.6 K in figure 10, there is only one relaxation peak,

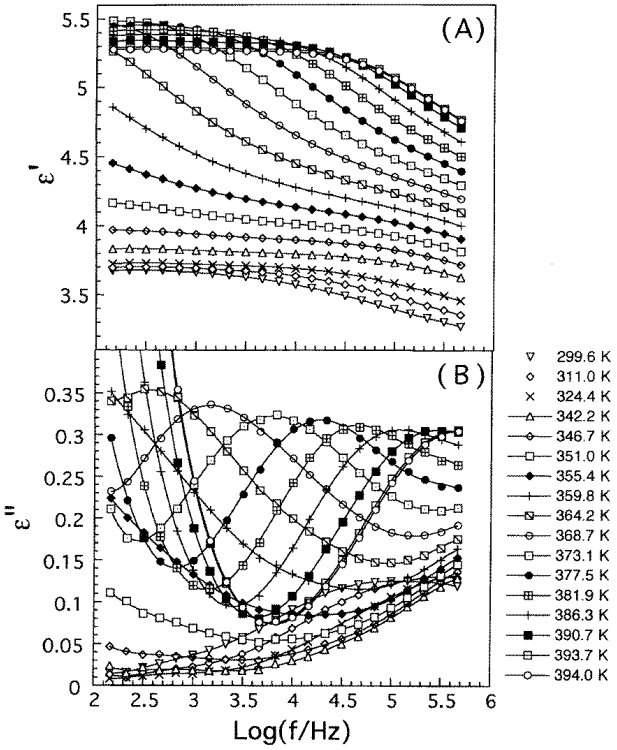

Figure 10. The permittivity and loss spectra of the completely polymerized form of the initially molecular mixture. The thermal treatment of the sample by means of which this state was achieved is described in the text, and in figure 1(A).

of height $\varepsilon'' = 0.13$, at frequency 0.1 MHz. This is the typical Johari–Goldstein relaxation process (we use this term here to maintain a distinction between this process and the sub-T_g relaxation process of the mode-coupling theory, as suggested and utilized in several review papers [49–52]), which shifts towards a higher frequency on heating the polymer, and a new, slower, α-relaxation process becomes evident at a lower frequency. Its peak also shifts towards a higher frequency on heating to 394 K. (Note that the two data sets at 393.7 K and 394.0 K, shown in figure 10, indicate the reproducibility of the data, and the sensitivity of the SITA assembly.) The low-temperature plateau value of ε', or ε_s for the Johari–Goldstein relaxation, is 3.66 at 299.6 K, and its spectra are too broad to allow determination of the corresponding ε_∞, whose value should be 2.6 or less, i.e., equal to the square of the infrared refractive index. ε_s for this process increases from 3.66 at 299.6 K to 4.5 at 351.0 K, and seems to increase further with increase in the temperature, as shown by the ε'-spectra at subsequently higher temperatures, where an approach towards a plateau-like value for ε_s is interrupted by the contribution to ε' from the α-relaxation process whose peak is moved out of the spectral window.

This indicates that the strength of the Johari–Goldstein relaxation process increases on heating and that of the α-relaxation process decreases until the magnitude of the latter becomes vanishingly small. At that temperature the two become just one relaxation process, and at higher temperatures the dynamics is that of the Johari–Goldstein relaxation process. A variety of earlier studies [52–54] have also shown that at high temperatures there is only

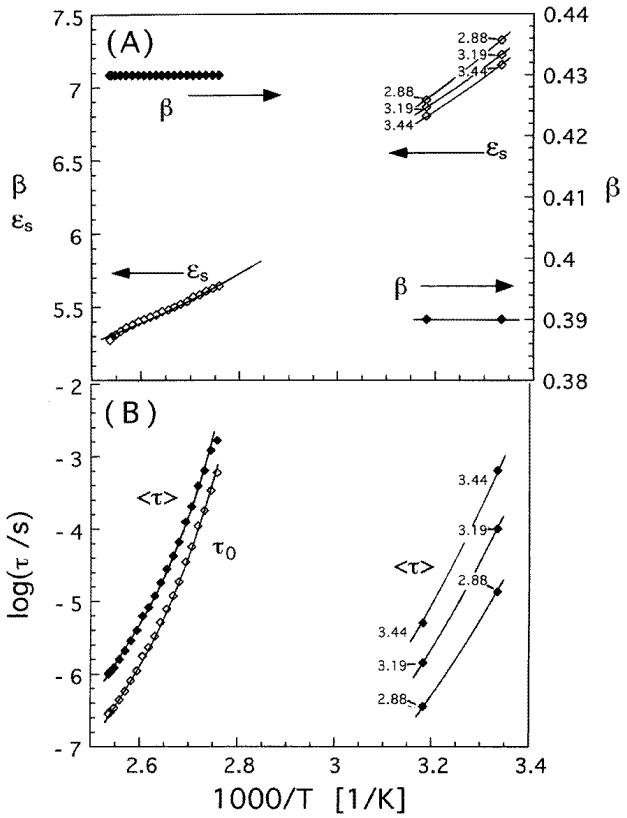

Figure 11. The equilibrium permittivity and β for the completely polymerized state are plotted against the reciprocal temperature in the top half, and the average dielectric relaxation time of this state ($n = 6.02 \times 10^{23}$) is plotted against the reciprocal temperature in the bottom half. For comparison, the data for certain values of n measured at 314.2 K here, and for the same values of n but measured at 299.8 K (unpublished study) are included. The numbers next to the data points are the values of $n/10^{23}$. Vertical arrows indicate the direction of change in the property with increase in n. Horizontal arrows point towards the labelling on the axis that relates to that property.

one relaxation process in liquids.

The ε'- and ε''-spectra of figure 10 were analysed to obtain the values of ε_s, β, and τ_0 at different temperatures in the same manner as in section 4.3. These values are plotted against the reciprocal temperature in figure 11. Also plotted are the corresponding values of ε_s, β, and τ_0 for values of $n < 6.02 \times 10^{23}$, as obtained from this study and at 299.8 K from another of our studies. It is remarkable that the value of β of 0.39 is about the same ($\beta = 0.38$) as for the partially polymerized samples, as given in table 1. This shows that after n has reached a value of 2.24×10^{23}, a further increase in n does not change the distribution of relaxation times. The distribution of the molecular environment, which seems to determine the value of β, remains effectively unchanged when the number of covalent bonds increases by as much as by a factor of 3. The characteristic relaxation time decreases with increase in the temperature in the manner described by the Vogel–Fulcher–Tammann equation, as is seen in figure 11. Because of the limited number of data available now, the parameters of this equation cannot be unambiguously determined.

5. Conclusion

When considered in terms of the number of covalent bonds in the structure of the macromolecules formed by polymerization of a liquid, the decrease in the configurational entropy, or equivalently the number of configurations accessible to the molecules, slows the dynamics of molecular diffusion, both translational and rotational, differently at different temperatures. An increase in temperature can restore the rate of this dynamics, but only when the structure is different, as characterized by the number of covalent bonds in it. The equilibrium behaviour, as indicated by the changes in the dipolar orientational correlation, and in the phonon frequencies, cannot be restored in the same manner.

The dc conductivity, which is initially determined by the viscosity of the polymerizing liquid, is ultimately controlled by the decrease in the population of ions, on decrease in the equilibrium permittivity. A new faster relaxation process, which is a reflection of the development of localized modes of motions in the otherwise rigid structure, evolves as polymerization continues. The dynamics of this relaxation does not change with further polymerization, but its strength increases towards a limiting value, and its distribution of relaxation times seems to remain constant.

Acknowledgment

GPJ is grateful for the hospitality of the IFAM del CNR group in Pisa, Italy, during his visit for carrying out these studies.

References

[1] Johari G P 1994 Dynamics of irreversibly forming macromolecules *Disorder Effects in Relaxational Processes* ed R Richert and A Blumen (Berlin: Springer) p 627
[2] Senturia S D and Sheppard N F Jr 1986 *Adv. Polym. Sci.* **80** 1
[3] Malkin A Y and Kulichikhin S G 1993 *Adv. Polym. Sci.* **101** 217
[4] Alig I, Lellinger D and Johari G P 1992 *J. Polym. Sci.* B **30** 791
and references 3 to 13 and 16 to 20 therein.
[5] Younes M, Wartewig S, Lellinger D, Strehmel B and Strehmel V 1994 *Polymer* **35** 5269
[6] Parthun M G and Johari G P 1992 *J. Polym. Sci.* B **30** 655
Parthun M G and Johari G P 1992 *Macromolecules* **25** 3254
[7] Aronhime M T and Gillham J K 1984 *Adv. Polym. Sci.* **78** 85
[8] McGettrick B P, Vij J K and McArdle C B 1994 *Int. J. Adhesion Adhesives* **14** 211
[9] Choy I-C and Plazek D J 1986 *J. Polym. Sci.* B **24** 1303
[10] Plazek D J and Frund Z N Jr 1990 *J. Polym. Sci.* B **28** 431
[11] Mangion M B M, Wang M and Johari G P 1992 *J. Polym. Sci.* B **30** 445
[12] Sidebottom D and Johari G P 1990 *Chem. Phys.* **147** 205
[13] Deng Y and Martin C G 1994 *J. Polym. Sci.* B **32** 2115
[14] Cassetari M, Salvetti G, Tombari E, Veronesi S and Johari G P 1993 *J. Mol. Liq.* **56** 141
Cassetari M, Salvetti G, Tombari E, Veronesi S and Johari G P 1993 *Physica* A **201** 95
Cassetari M, Salvetti G, Tombari E, Veronesi S and Johari G P 1994 *J. Non-Cryst. Solids* **172–174** 554
[15] Tombari E and Johari G P 1992 *J. Chem. Phys.* **97** 6677
[16] Parthun M G and G P Johari 1995 *J. Chem. Phys.* **102** 6301
Parthun M G and G P Johari 1995 *J. Chem. Phys.* **103** 440
[17] Wasylyshyn D A and Johari G P 1996 *J. Chem. Phys.* **104** 5683
[18] Ferrari C, Salvetti G, Tombari E and Johari G P 1996 *Phys. Rev.* E **54** R1058
[19] Barton J M 1985 *Adv. Polym. Sci.* **72** 111
[20] Cassetari M, Salvetti G, Tombari E, Veronesi S and Johari G P 1993 *J. Polym. Sci.* B **31** 205
[21] Cassetari M, Papucci F, Salvetti G, Tombari E, Veronesi S and Johari G P 1993 *Rev. Sci. Instrum.* **64** 1076
[22] Johari G P, Wasylyshyn D A, Salvetti G and Tombari E 1997 *J. Chem. Phys.* at press

[23] Johnson J F and Cole R H 1951 *J. Am. Chem. Soc.* **73** 4536
[24] Cole R H and Tombari 1991 *J. Non-Cryst. Solids* **131–133** 969
[25] Huang P N and Johari G P 1993 *J. Mol. Liq.* **56** 225
[26] Parthun M G and Johari G P 1995 *J. Chem. Soc. Faraday Trans.* **91** 329
[27] Mangion M B M and Johari G P 1991 *J. Polym. Sci.* B **29** 1127
Mangion M B M and Johari G P 1991 *J. Non-Cryst. Solids* **131–133** 921
[28] Casalini R, Corezzi S, Fioretto B, Livi A and Rolla P A 1996 *Phys. Rev.* B **53** 564
[29] Djabourov M 1988 *Contemp. Phys.* **29** 273
[30] Stauffer D, Coniglio A and Adam M 1982 *Adv. Polym. Sci.* **44** 105
[31] Wasylyshyn D A and Johari G P 1996 *J. Polym. Sci.* B **35** 437
[32] Wasylyshyn D A, Parthun M G and Johari G P 1996 *J. Mol. Liq.* **69** 219
[33] Davies C W 1962 *Ion Association* (London: Butterworths)
[34] Mijovic J and Andjelic S 1995 *Macromolecules* **28** 2787
[35] Parthun M G and Johari G P 1993 *Macromolecules* **26** 2392
[36] Pathmanathan K and Johari G P 1988 *Polymer* **29** 303
[37] Onsager L 1936 *J. Am. Chem. Soc.* **58** 1486
[38] Kirkwood J G 1939 *J. Chem. Phys.* **7** 911
[39] Fröhlich H 1958 *Theory of Dielectrics* 2nd edn (Oxford: Oxford University Press)
[40] Hodge I M and Berens A R 1982 *Macromolecules* **15** 762
[41] Sartor G, Mayer E and Johari G P 1994 *J. Polym. Sci.* B **32** 683
[42] Sartor G and Johari G P 1996 *J. Phys. Chem.* **100** 10 450
[43] Rudisser S, Hallbrucker A, Mayer E and Johari G P 1996 *J. Phys. Chem.* **101** 266
[44] Butta E, Livi A, Levita G and Rolla P A 1995 *J. Polym. Sci.* B **33** 2253
[45] Parthun M G, Wasylyshyn D A and Johari G P 1996 *J. Mol. Liq.* **69** 283
[46] Adam G and Gibbs J H 1965 *J. Chem. Phys.* **43** 139
[47] Alig I and Johari G P 1993 *J. Polym. Sci.* B **31** 299
[48] Cavaille J Y, Perez J and Johari G P 1989 *Phys. Rev.* B **39** 2411
[49] Angell C A 1995 *Science* **267** 1924
[50] Frick B and Richter D 1995 *Science* **267** 1939
[51] Ediger M D, Angell C A and Nagel S R 1996 *J. Phys. Chem.* **100** 13 200
[52] Nagel S R 1993 *Phase Transitions and Relaxations in Systems with Competing Energy Scales* ed T Riste and D Sherrington (Dordrecht: Kluwer) p 259
[53] Wu L and Nagel S R 1992 *Phys. Rev.* B **46** 11 198
[54] Rossler E 1990 *Phys. Rev. Lett.* **65** 15 955